

Linking Blazar Light Curves at 1 mm to Higher Frequencies: Intraday Variations Parsecs from the Black Hole



Alan P. Marscher

Institute for Astrophysical Research, Boston University; marscher@bu.edu



SUMMARY

Common astronomical folk lore places optical to γ -ray emission in blazars close to the black hole and radio emission much farther out. While the latter is generally true at cm wavelengths, it is often untrue at millimeter wavelengths. A particularly noteworthy event was the November 2010 mega-outburst in the quasar 3C 454.3 (see Fig. 2). The 1 mm flux measured by the SMA exhibited a sharp flare that was essentially simultaneous with an equally sharp optical and gamma-ray flare. Optical depth arguments place the event parsecs from the black hole. Such extremely rapid, intraday variability on parsec scales needs a new paradigm. One contender, the author's new TEMZ model involving turbulent plasma crossing shocks, is presented here.

This presentation shows some examples of well-sampled monitoring observations of multi-wavelength flux and radio-optical polarization of blazars. The TEMZ model explains the variability patterns through magnetic turbulence, with particle acceleration that depends on the angle between the local magnetic field of a turbulent cell and shock fronts that might be present. The model is potentially capable of explaining the complex behavior of these enigmatic galactic nuclei, which are the most luminous long-lived objects in the universe.

Time Variations of Non-thermal Emission in Blazars

Observations: As illustrated in Figures 1-2, the flux and polarization of blazars is highly variable. The linear polarization often fluctuates in an apparently random manner. In addition, the mean level of polarization is lower, and the fluctuations less pronounced, at longer wavelengths. Flares in the 1 mm flux, produced on parsec scales, are sometimes simultaneous with optical and γ -ray flares, as in 3C 454.3 in Nov 2010.

Interpretation: The seemingly random variations in polarization can occur if the relativistic plasma flowing down the jet of the blazar is magnetically turbulent. A crude model involves N radiating cells, each with a uniform but randomly oriented magnetic field. The mean degree of polarization is then $\langle p \rangle \sim 75\% N^{-1/2}$ and the standard deviation is $\sim \langle p \rangle / 2$ (Burn 1966, MNRAS, 133, 67). An observed value $\langle p \rangle \sim 15\%$ therefore implies that ~ 25 cells are involved in the emission. The number of cells needed increases if there is partial ordering of the field, e.g., by a shock or velocity shear.

Turbulent fields can accelerate relativistic particles via the 2nd-order Fermi mechanism. They can also create the conditions for magnetic reconnections at sites where oppositely directed field lines meet. This should result in more efficient particle acceleration via a 1st-order process, but its affect on the polarization has yet to be calculated.

Stationary emission features – such as the “VLBI core” seen at one end of a blazar jet on mm-wave VLBI images (see Fig. 3, which reveals 3 such features in BL Lac) – can be described as standing “recollimation” shocks (Cawthorne et al. 2013, ApJ, 772, 14; Cohen et al. 2014, ApJ, 787, 151). Relativistic particles accelerated in the turbulent flow will gain energy as they cross such a shock, either by compressive heating or, if the field lines are nearly parallel to the shock normal, 1st-order Fermi acceleration.

Based on these considerations, the author proposes a model to explain much of the observed behavior of blazars out to parsec scales.

1. The jet is accelerated to relativistic flow speeds and collimated to within 1° or less by a tight helical magnetic field.
2. As the plasma energy density approaches equipartition with the magnetic energy density, current-driven instabilities render the flow turbulent. Particle acceleration via the 2nd-order Fermi mechanism radiation leads to synchrotron and inverse Compton radiation.
3. Pressure mismatches with the external medium create cone-shaped “recollimation” shocks that are seen as stationary emission features at mm wavelengths. Electrons are further energized by the shock, especially in cells where the magnetic field lines are nearly parallel to the shock normal. Only a small number of cells have electrons at energies $> 5000 m c^2$ that radiate at optical & γ -ray frequencies.
4. The smaller emission volumes cause variations in the optical & γ -ray flux to be more pronounced than at lower frequencies. For the same reason, the larger number of emitting cells at lower frequencies leads to lower mean polarization and steadier polarization position angles.
5. Major outbursts, flares, periods of relative quiescence, and minor variations in the emission occur from millimeter to γ -ray wavelengths as the physical parameters of the flow vary from the turbulence and also possibly from random fluctuations in the rate of input of energy density into the flow. There is a correlation between pairs of wavebands, with varying strength and time lag.

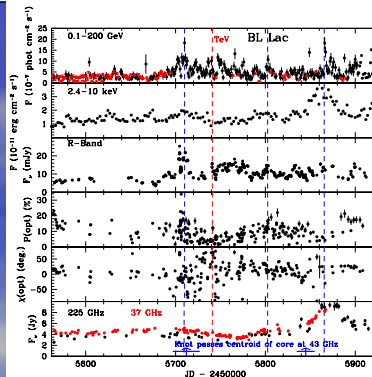


Fig. 1a: Flux and polarization curves of BL Lac during 2011, from Arlen et al. (2013, ApJ, 762, 92) and Marscher et al. (in prep.).

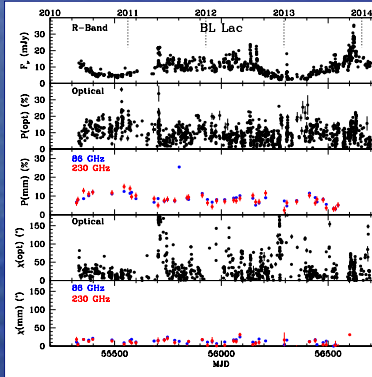


Fig. 1b: Four-year linear polarization curves of BL Lac at optical and millimeter wavelengths. Top panel contains optical light curve. Note the lower mean degree of mm-wave polarization and lower level of fluctuations compared with the optical behavior.

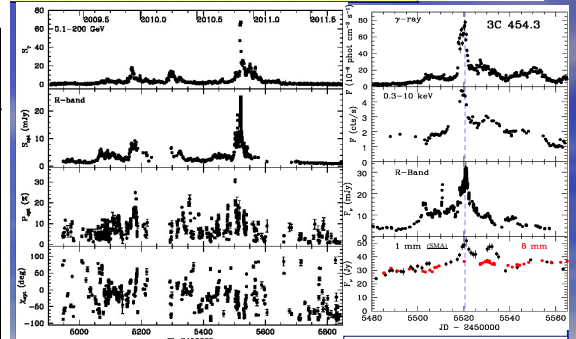


Fig. 2a: Flux and polarization curves of 3C 454.3 from Jorstad et al. (2013, 773, 147). Much of the data are also published in Wehrle et al. (2012, ApJ, 758, 72).

Fig. 2b: Blow-up of late-2010 outburst. Note that main flare was simultaneous from 1 mm to γ -ray wavelengths. Data from Wehrle et al. (2012, ApJ, 758, 72).

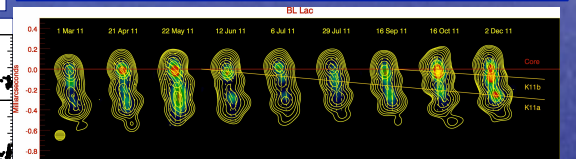


Fig. 3a (above): Sequence of 43 GHz VLBA images of BL Lac in 2011. Note 3 quasi-stationary features: core (northernmost), and 2 others. Superluminal emission features are most easily recognized in polarization (color, with white sticks showing electric vector).

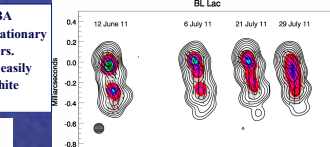
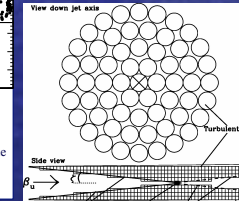


Fig. 3b (above): Sequence of 43 GHz VLBA images of BL Lac near TeV gamma-ray flare on 28 June 2011, from Arlen et al. (2013). Enhanced plasma passed through the quasi-stationary features during the flaring period.

Fig. 4 (left): Sketch of the author's numerical model for blazar emission from turbulent plasma crossing a standing cone-shaped shock.

Turbulent Extreme Multi-Zone (TEMZ) Numerical Model (Marscher 2014, ApJ, 780, 87)

Figure 4 sketches the geometry of a numerical model that incorporates the physical features outlined in the text panel to the left. Each of the many computational cells – typically 169 across the jet and up to 400 in the longitudinal direction – contains a turbulent cell (with uniform properties), which move downstream by one computational cell during each time step. The fluctuating components of the magnetic field and relativistic electron density are selected randomly at the boundaries of 3-D zones of different sizes (single cell, 2 cells on a side, 4 cells per side, and 8 cells per side) with the zones contributing to the field and density variations in proportion to the zone size raised to the 1/3 power, following a Kolmogorov spectrum. The level of the fluctuations is a free parameter, usually assumed to be $\sim 50\%$ as in the solar wind.

The relativistic electrons are given a power-law energy distribution that is amplified by the shock, beyond which the electrons lose energy from synchrotron and inverse Compton radiation. (Adiabatic cooling is insignificant across the computational grid.) For cells with field directions nearly parallel to the shock normal (the “subluminal” case of diffusive particle acceleration), electrons attain the highest energies, and therefore can radiate at the highest frequencies. This plus the energy losses limit the volume of high-frequency emission. Some sample flux and polarization vs. time curves are displayed in Figure 5 below:

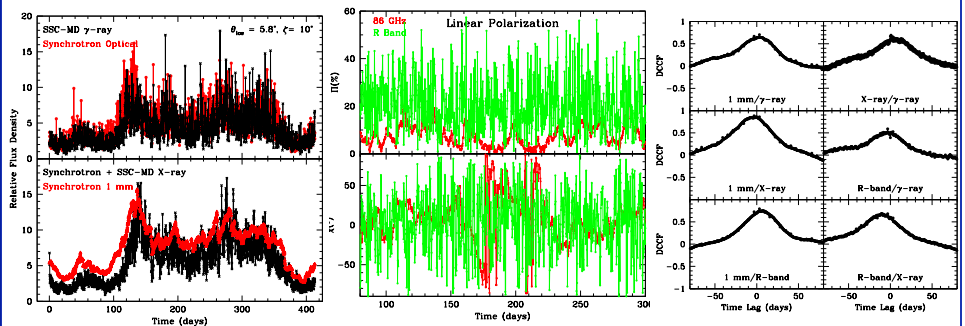


Figure 5. Sample output of the TEMZ code for a simulated blazar with physical parameters similar to BL Lac. Although the output is not identical to the BL Lac data, the similarities are encouraging. *Left:* Light curves at 4 different wavebands; note that the variations are smoother at lower frequencies. Note also that intra-day variations often occur at all wavebands. *Center:* Linear polarization vs. time; note that $\langle p \rangle$ is lower and that both $\langle p \rangle$ and the position angle vary more smoothly at the lower frequency. *Right:* Correlations of flux variations between various wavebands; note time delays and different strengths of the correlations.

Acknowledgements: This research has been supported in part by NASA through Fermi guest investigator grants NNX11AQ03G, NNX12AO79G, & NNX13AP06G.